Published in final edited form as:
Nat Neurosci. 2007 December ; 10(12): 1594–1600.

Defining Cortical Frequency Tuning with Recurrent Excitatory Circuitry

Baohua B. Liu[1,2,*], **Guangying K. Wu**[1,3,*], **Robert Arbuckle**[1,#], **Huizhong W. Tao**[1,4], and **Li I. Zhang**[1,2]

1 *Zilkha Neurogenetic Institute, University of Southern California*

2 *Department of Physiology & Biophysics, University of Southern California*

3 *Neuroscience Graduate Program, University of Southern California*

4 *Department of Ophthalmology, and Keck School of Medicine, University of Southern California*

Abstract

Neurons in the recipient layers of sensory cortices receive excitatory input of two major sources: the feedforward thalamocortical and recurrent intracortical inputs. To address their respective functional roles, we developed a novel method to silence cortex by activating $GABA_A$ while blocking $GABA_B$ receptors. In the rat primary auditory cortex, *in vivo* whole-cell recording from the same neuron before and after local cortical silencing revealed that thalamic input occupies the same area of frequency-intensity tonal receptive field as the total excitatory input, but exhibits a flattened tuning curve. In contrast, excitatory intracortical input is sharply tuned, with a tuning curve closely matching that of suprathreshold responses. This can be attributed to a selective amplification of cortical cells' responses at preferred frequencies by intracortical inputs from similarly tuned neurons. Thus, weakly-tuned thalamocortical inputs determine the subthreshold responding range, while intracortical inputs largely define the tuning. Such circuits may ensure a faithful conveyance of sensory information.

Although many aspects of representation/processing function of neurons in the recipient layers of cortex appear to reflect converging thalamocortical inputs[1–5], the functional role and the underlying pattern of thalamocortical and, in particular, intracortical excitatory inputs remain unsolved[6–9]. Extensive efforts have been made to understand the thalamocortical contribution to cortical responses. These previous studies can be mostly categorized into two types: 1) directly compare the response properties between simultaneously recorded neurons in the thalamus and cortex [1,10–12]; and 2) isolate thalamocortical input by preventing spiking of cortical neurons[2,13–17]. The first type of studies mostly used extracellular recordings, and identified putatively connected thalamic and cortical units based on temporal correlation between their spikes. This approach provides information on the tuning properties of individual thalamic and cortical neurons as well as the nature of connection between them. A recent study in the somatosensory cortex[5], by pairing extracellular recording of thalamic neurons with intracellular recording of cortical cells, suggests that cortical neurons receive a number of weak but synchronously activated thalamic inputs, which exhibit similar tuning properties as the recorded cortical neuron. However, since the pattern underlying divergent output connections made by a single thalamic neuron, or convergent thalamic inputs made on a single cortical

Correspondence should be addressed to: L.I.Zhang (liizhang@usc.edu), Phone: 323-442-4347.
*These authors contributed equally to this study
#Present address: New York University School of Medicine

Author Contributions

L.Z. conceived the study. G.W. and B.L. performed *in vivo* experiments and data analysis. B.L. modeled the effects of cocktail application on synaptic responses. R.A. was involved in current-clamp recordings. L.Z. and H.T. supervised the project and wrote the paper.

neuron, remains largely unknown, it is difficult to determine the respective functional roles of thalamocortical and intracortical inputs.

The second approach depends on an effective silencing of the cortex without affecting thalamocortical transmission. Three methods have been previously used to silence the cortex: 1) cortical application of muscimol, an agonist of $GABA_A$ receptors, to prevent neuronal spiking[13–15]; 2) cooling the cortex (4–14 °C) to block spike generation in neurons[2,17,18]; 3) electrical stimulation of the cortex to produce a long inhibition widow (>100 ms) following excitation, during which spikes cannot be generated[16]. However, all these methods are expected to have impacts on thalamocortical presynaptic transmission. Electrical stimulation can result in complex presynaptic effects such as short-term depression or facilitation. Although the mechanism underlying cooling-induced action potential block is not yet clear, it is likely that both the action potential spread in axons and presynaptic vesicle release will also be affected by a drastic temperature decrease. Microinjection, iontophoresis or perfusion of muscimol have more often been applied to silence intracortical connections [13–15]. It was assumed that muscimol was a highly specific agonist to $GABA_A$ receptors. However this view has been challenged by recent findings that muscimol at a relatively low concentration can already activate $GABA_B$ receptors, and reduce synaptic transmission through presynaptic $GABA_B$ receptors [19].

In this work, we developed a new pharmacological method to silence the cortex. By simultaneously blocking $GABA_B$ receptors with a specific antagonist, we could largely prevent the non-specific effect of muscimol on presynaptic transmission. By applying *in vivo* whole-cell voltage-clamp recording in the rat primary auditory cortex (A1), we examined tone-evoked synaptic responses in layer 4 neurons before and after local cortical silencing. We found that thalamocortical inputs determine the area of synaptic frequency-intensity tonal receptive field (TRF), while intracortical excitatory inputs largely define the frequency tuning by selectively amplifying responses at preferred frequencies of the cortical cell.

Results

Silencing cortex with muscimol and SCH50911 cocktail

To understand how thalamocortical and intracortical synaptic inputs contribute to the processing of individual cortical neurons respectively, we developed a cocktail pharmacological method to effectively silence intracortical connections while largely preserving thalamocortical synaptic transmission. Previously, cortical application of muscimol, a $GABA_A$ receptor agonist, had been used to prevent spiking of cortical neurons[13–15]. However, recent studies suggest that muscimol can activate $GABA_B$ receptors at a relatively low concentration (EC_{50} = 25μM) [19]. Since $GABA_B$ receptors exist on thalamocortical axons, cortical muscimol application will result in a significant reduction of evoked transmitter release from these axons [20]. As shown in Fig. 1a, cortical microinjection of muscimol, or a specific agonist of $GABA_B$ receptors, baclofen, largely eliminated tone-evoked field potentials recorded in the cortex. To overcome the non-specific effect of muscimol on presynaptic transmission, we applied SCH50911, a specific antagonist of $GABA_B$ receptors, together with muscimol. This significantly restored the magnitude of tone-evoked field potentials (Fig. 1a). Application of SCH50911 alone slightly increased the amplitude of field potential responses (Fig. 1a) and prolonged tone-evoked spiking activity (Supplementary Fig. 1), but did not change the shape of spike TRFs of cortical neurons (Supplementary Fig. 1). This is consistent with the late, prolonged inhibition mediated by postsynaptic $GABA_B$ receptors.

Considering the competitive binding between muscimol/SCH50911 and $GABA_A$/$GABA_B$ receptors, we derived an optimized concentration ratio for the co-applied SCH50911 and

muscimol (1.5:1) to achieve an effective activation of $GABA_A$ receptors and blockade of $GABA_B$ receptors (see Methods and Supplementary Information Part 1 for detailed calculation). After slowly injecting about 10–20 nano-litters of the cocktail solution into the cortex, firing of cortical cells within a horizontal distance of 500 μm was effectively blocked (spike count reduced by >95%), as indicated by the extracellular multi-unit recordings (Fig. 1b). This effect can last for at least 3 hours (data not shown). Since the highest density of local intracortical excitatory input comes from neurons within a 500 μm radium [6,21,22] and the size of rat A1 is about 1–2 mm^2 (Ref.23), we believe that this local injection method is effective in silencing the majority of intracortical connections, although some long-distance connections may not be affected. As a control, when the cortex was injected with the vehicle solution (artificial cerebrospinal fluid, or ACSF), no significant effect was observed on tone-evoked cortical field potentials (data not shown).

To examine the effect of local cortical silencing on receptive field properties of single cortical neurons, *in vivo* whole-cell voltage-clamp recordings were performed on excitatory pyramidal neurons in layer 4 of A1 (premapped with extracellular recording, see Methods), shortly after cortical injection of muscimol or the mixture of muscimol and SCH50911. Excitatory synaptic responses evoked by pure tones of various frequencies and intensities were recorded with the neuron clamped at −70 mV. The excitatory synaptic TRF was reconstructed after the recording. In muscimol treated cortices, only traces of synaptic responses were observed within a small tonal responsive area (Fig. 1c, left). On the contrary, in cocktail treated cortices excitatory synaptic responses with large amplitudes were observed (Fig. 1c, right). The bandwidth of excitatory synaptic TRF measured at 60dB sound pressure level (SPL), BW60, was not significantly different from that observed in control A1 where ACSF solution was injected (Fig. 1d), or in normal A1. The local silencing of A1 under our experimental condition did not affect response properties in the auditory thalamus that projects to A1, as multi-unit spike TRFs in the ventral division of the medial geniculate body (MGBv) remained similar after cortical injection of the cocktail (Fig. 1e, f). This well-restricted drug effect in the cortex may be attributed to the small volume of drug application in our experiments. The above population studies suggest that the shape of excitatory synaptic TRF of neurons in the input layers of A1 is primarily determined by thalamocortical input. The apparently reduced bandwidth of excitatory synaptic TRF in the presence of muscimol (Fig. 1d, also see Ref. 14) may be largely attributed to the nonspecific effect of muscimol on presynaptic $GABA_B$ receptors.

Thalamocortical input determines the area of synaptic TRF

To further examine the pattern of thalamocortical and intracortical excitatory inputs, and their roles in determining frequency tuning, we recorded synaptic TRFs from the same A1 neuron before and after cortical silencing. An example of such recording is shown in Fig. 2. The cell was clamped at −70 mV and then 0 mV to record tone-evoked excitatory and inhibitory currents, respectively (Fig. 2a). The linearity of the I–V curve suggests that the cell was reasonably clamped (Fig. 2b, see Methods and Supplementary Information Part 2 for detailed discussion). The injection of the cocktail was made at a cortical site about 500 μm below the pial surface and 100 μm horizontally away from the recorded cell. After the injection, tone-evoked inhibitory currents were eliminated (Fig. 2a), consistent with the silencing of intracortical inhibitory connections. The amplitude of excitatory currents was significantly reduced (Fig. 2a), which can be attributed to two factors: silencing of intracortical excitatory connections and nonspecific effects of cocktail application including those caused by changes in series resistance and input resistance (see Supplementary Information Part 2 for detailed calculation). We assumed that tone-evoked excitatory responses at the subthreshold intensity threshold (20 dB in this particular cell) were mostly contributed by monosynaptic thalamocortical inputs. This is supported by three observations. First, the reduction in the amplitude of excitatory currents was the smallest at the subthreshold intensity threshold.

Second, the multi-unit spike TRF recorded from the same site before silencing had a higher intensity threshold (30 dB, Supplementary Fig. 2), suggesting that the synaptic currents at the subthreshold intensity threshold are unlikely contributed by local intracortical inputs. Third, the kinetics of the rising phase of response currents at the intensity threshold remained mono-phased after cocktail application, while that of response currents to best-frequency tones above the intensity threshold changed from bi-phased to mono-phased, consistent with synaptic inputs of two sources that have different onsets (Fig. 2d, I–IV). Thus, based on the relative change in the amplitude of average response at the intensity threshold after the cocktail application (−29%), we estimated that the cocktail application had caused a 29% nonspecific reduction of the response amplitude in this cell (see Supplementary Information Part 2 for more discussion). The amplitude of each excitatory response after cortical silencing was then corrected by a factor of 1/0.71. The excitatory TRF after the correction is shown by the bottom color map in Fig. 2d. It is apparent that after cortical silencing, there is no significant change in the range of responding frequencies at various testing intensities, or in the intensity threshold (Fig. 2d). This result further supports the notion that thalamocortical input primarily defines the shape of excitatory synaptic TRF. In addition, the graded amplitude of thalamocortical responses indicates that the cortical neuron is innervated by a number of thalamic neurons, with each of them possessing spike TRFs within the frequency-intensity range defined by the excitatory synaptic TRF of this cell.

We next examined the onset latency for each response in the TRF before and after cortical silencing (Fig. 2e). A clear pattern of onset-latency values was observed in the TRF, with the shortest latencies appearing at high intensities and clustering around preferred frequencies, and the longest latencies appearing at the periphery of the TRF. This is reminiscent of a similar finding on visual cortical receptive fields[24], based on which it was proposed that long-latency responses are due to intracortical spread of visual activity. However, in the present study, there were no significant changes in either short or long onset-latencies after cortical silencing (Fig. 2f), suggesting that the onset latency is determined mostly by thalamocortical input. The variation in onset latency is likely due to variation in the conduction velocity subcortically as well as in the integration time for action potential generation in subcortical neurons.

Weakly tuned thalamic and sharply tuned intracortical input

The analysis above indicates that thalamocortical input primarily determines the area of synaptic TRF. We next examined the role of thalamic and intracortical inputs in determining cortical frequency tuning. Intracortical connections provide both excitatory and inhibitory inputs. Previous data have suggested that intracortical inhibitory inputs can sharpen spike tuning curves through an analogous “iceberg” effect [25–27], and that they may also increase the temporal precision of spike responses by temporally following excitatory inputs with a brief delay [26]. On the other hand, the functional role of intracortical excitatory inputs remains largely unknown. Here, we compared the frequency tuning curves before and after cortical silencing, which are depicted by the envelope of amplitudes of responses at certain intensity. It appears that the shape of the tuning curves becomes more flattened after cortical silencing, as reflected by an increase in the half-peak bandwidth of the tuning curves (Fig. 2g, h). The flat or plateau peak of thalamocortical tuning curve (Fig. 2g) indicates that thalamocortical input is in fact weakly tuned.

A total of five cortical neurons were examined in the above manner (another four cells are shown in Fig. 3). In all of these neurons, after cortical silencing there was no significant change in the range of responding frequencies or in the intensity threshold (Fig. 3a, c, e, g, j, Supplementary Fig. 3). At the mean time, the frequency tuning curve became flattened, exhibiting a broad plateau peak that covers the preferred frequencies of the cell and a broader half-peak bandwidth than that of total input (Fig. 3b, d, f, h, i, j). We further quantified the

pattern of intracortical excitatory input by subtracting the thalamocortical component from the total excitatory responses (Fig. 2h, 3b, d, f, h, black lines). The tuning curves for excitatory intracortical input exhibited the same preferred frequencies as those for total excitatory input, but their half-peak bandwidths were significantly narrower than those for both the total and thalamocortical inputs (Fig. 3i). These results demonstrate that local intracortical excitatory input is more sharply tuned than thalamocortical input, and contributes most at the preferred frequencies of the cell.

Recurrent excitation largely defines frequency tuning

What is the role of intracortical input in determining the frequency tuning of cortical cells? The preferred frequencies of intracortical excitatory input closely matched the plateau peak of thalamocortical tuning curve (Fig. 2g, 3b, d, f, h), suggesting that the intracortical inputs arised from a group of similarly tuned neurons. We further carried out whole-cell current-clamp recordings to compare subthreshold and spike TRFs in the same cortical neuron. We found that the frequency range for spike responses was significantly narrower than that for excitatory synaptic input (Fig. 4a, 4b). The average frequency range for spike responses measured at 60dB is about 54 ± 7% (mean ± s.d., n = 10) of that for excitatory synaptic input, consistent with previous findings that spike threshold sharpens neuronal tuning for many stimulus attributes[27–31]. As a result, each intracortical excitatory input, which depends on a cortical cell's firing, will inevitably have a narrower frequency range than direct thalamocortical input. When excitatory intracortical inputs with similar tuning properties are pooled, they can selectively amplify excitatory responses at their preferred frequencies.

We next compared the contribution of thalamocortical and intracortical inputs to synaptic tuning curve over the frequency range of suprathreshold responses, which reflects the spiking probability of the cell under fluctuating membrane potentials. The suprathreshold response range was estimated by the derived membrane potential responses (based on synaptic responses before cortical silencing, see Methods) that exhibited an increase of larger than 20 mV. The tuning curves of the total, the thalamocortical as well as the derived intracortical inputs were then thresholded within the defined suprathreshold frequency range, and were normalized. The bandwidths of these thresholded tuning curves were compared. As shown in Fig. 4c, within the suprathreshold frequency range, the tuning curve of intracortical input matched well with that of total excitatory input. In contrast, the thalamocortical tuning curve was significantly broader. This finding further supports the notion that although thalamocortical input determines the subthreshold responding range, the frequency tuning of the cortical neuron is largely defined by more narrowly tuned intracortical excitatory input.

Discussion

Extensive efforts have been made to address the role of feedforward thalamocortical input in determining the response properties or the representation/processing function of layer 4 neurons in the sensory cortex [1–5]. Experimental studies in the primary visual, somatosensory and auditory cortices all suggest that the response properties of layer 4 cortical neurons can be explained by the convergence of thalamic inputs[1–5, 9, 32]. However, the extent to which response properties of cortical neurons represent those of thalamic inputs, and the functional pattern of these inputs have not been fully addressed. Moreover, the contribution of recurrent intracortical excitatory connections to cortical processing remains largely unclear. Modeling studies suggest that they may function as a cortical amplifier for the feedforward excitation [6], and may account for the emergence of contrast-invariant orientation selectivity in the visual cortex [7]. In contrast, the recent study in the somatosensory cortex suggests that cortical amplification may not be required since layer 4 neurons receive a large number of synchronous

sensory-driven thalamic inputs, which together can be strong enough to trigger spike responses[5].

In the present study, by using a cortical silencing method that leaves thalamocortical transmission largely unaffected, we were able to isolate the thalamocortical component underlying synaptic TRFs of cortical neurons. We conclude that thalamocortical input determines the range of subthreshold responses, since synaptic TRFs cover the same area before and after cortical silencing, although the amplitude of each excitatory response is reduced. This reduction can be attributed to the silencing of intracortical excitatory connections and non-specific effects caused by the cocktail application (see Supplementary Information Part 2 for detailed discussion). By taking into account the non-specific reduction and correcting response amplitudes accordingly, we estimate that for the largest tone-evoked excitatory response (saturating response) within the TRF, about 61 ± 11 % (mean ± s.d.) component is of thalamocortical origin and 39 ± 11% component of cortical origin (n = 5 cells). These values are comparable to the estimation in the cat primary visual cortex that thalamic input comprises about 46% of the total excitatory input [16]. The smallest tone-evoked responses after cortical silencing are presumably contributed by single thalamic inputs, and they can generate membrane depolarization of about 0.5 – 1 mV. We can thus estimate that each saturating response evoked by a pure tone stimulus consists of 18 ± 6 synchronous thalamic inputs (averaged from the five cells), consistent with the findings in the somatosensory cortex that many synchronous thalamic inputs are underlying sensory-evoked responses of single cortical neurons [5]. Although we could not infer the total number of thalamic projections made onto an A1 neuron, the excitatory TRF after cortical silencing has revealed a functional pattern of thalamic inputs.

The comparison between the tuning curves of total excitatory input, thalamocortical input and derived intracortical input revealed that weakly tuned thalamocortical input has been significantly sharpened by intracortical input. The peak of thalamocortical tuning curve is broad and flat, suggesting a low level of selectivity if responses at the peak are suprathreshold. The tuning curve of intracortical input is sharper, and the tuning curve of total excitatory input within the spiking frequency range resembles more to that of intracortical input than thalamocortical input. If we consider synaptic tuning curve as a distribution of spiking probability, we can conclude that intracortical input defines the shape of spike tuning curve, in a manner similar to adding a pyramid on top of a flat base (Supplementary Fig. 4). In other words, intracortical input “reconstitutes” the sharpness of frequency tuning in the cortex. The similar preferences of thalamacortical and intracortical tunings imply a recurrent circuitry in which local similarly tuned neurons excite each other (Supplementary Fig. 4). These intracortical inputs selectively amplify the thalamocortical signal and determine the optimal stimulus of the cortical cell. In conclusion, our results are consistent with models in which intracortical recurrent excitation determines stimulus selectivity of cortical neurons. We propose that by combining the breadth of feedforward excitation and selectivity of recurrent excitation, a reliable and faithful conveyance of subcortically processed sensory information to the cortex can be ensured.

Methods

Animal preparation and extracellular recording

All experimental procedures used in this study were approved by the Animal Care and Use Committee at the University of Southern California. Experiments were carried out in a sound-proof booth (Acoustic Systems) as described previously [23,27,33]. Female Sprague-Dawley rats about 3 months old and weighing 250–300g were anaesthetized with ketamine and xylazine (see discussion in Supplementary Information Part 2). Pure tones (0.5–64 kHz at 0.1 octave intervals, 25-ms duration, 3ms ramp) at eight 10 dB-spaced sound intensities were delivered

to the contralateral ear. Multiunit spike responses were recorded with parylene-coated tungsten microelectrodes (2 MΩ, FHC) at 500–600 μm below the pial surface. The number of tone-evoked spikes was counted within a window of 10–30 ms from the onset of tone stimulus. Auditory cortical mapping was carried out by sequentially recording from an array of cortical sites. The location of A1 was identified as previously described[23,27,33]. For recording in the auditory thalamus, we systematically mapped the medial geniculate body (MGB) with extracellular recordings in a 3-D manner by varying the depth and x-y coordinates of the electrode. We identified the ventral division of MGB (MGBv), which projects to A1[34], according to its tonotopy of frequency representation and the relatively sharper spike TRFs than other MGB divisions[35].

Local cortical silencing

Muscimol can activate both $GABA_A$ (EC_{50} = 1.7 μM) and $GABA_B$ (EC_{50} = 25 μM) receptors [19]. For effective silencing of the cortex with minimum impact on presynaptic transmission, we derived an optimized concentration ratio for muscimol and SCH50911 based on their competitive binding to $GABA_A$ or $GABA_B$ receptors:

$$A+Gb \xrightarrow{Kb_1} A\cdot Gb[A\cdot Gb]=[A]\times[Gb]\times[Kb_1] \quad (1)$$

$$B+Gb \xrightarrow{Kb_2} B\cdot Gb[B\cdot Gb]=[B]\times[Gb]\times[Kb_2] \quad (2)$$

$$A+Ga \xrightarrow{Ka_1} A\cdot Ga[A\cdot Ga]=[A]\times[Ga]\times[Ka_1] \quad (3)$$

$$B+Ga \xrightarrow{Ka_2} B\cdot Ga[B\cdot Ga]=[B]\times[Ga]\times[Ka_2] \quad (4)$$

A: SCH90511; B: muscimol; Gb: $GABA_B$ receptor; Ga: $GABA_A$ receptor.

Here, EC_{50} or IC_{50} values are used to calculate binding constants to reflect the functional effects of binding on channel opening or blocking: Kb_1=1/(1μM), Kb_2 = 1/(25μM), $Ka_1 \leq$1/(900μM), Ka_2=1/(1.7μM). We consider ≤5% receptors bound as no significant effect, and ≥ 95% as fully effective. Under these conditions, a ratio of 1.5:1 (SCH50911 : muscimol) was chosen (see Supplemental Information Part 1 for detailed calculation). A high concentration (6mM: 4mM) was used to effectively silence a relatively large cortical region. Pharmacological reagents (dissolved in ACSF solution containing Fast Green) or control solution (ACSF containing Fast Green) was injected through a glass micropipette with a tip opening of about 2–3 μm in diameter, attached via polyethylene tubing to a syringe. The pressure inside the tubing was monitored with a pressure gauge. After premapping A1, the pipette was inserted to 500–600 μm beneath the cortical surface at around the center of A1, controlled by a motorized micromanipulator. Injection was under a pressure of 3–4 psi and continued for 5 minutes. The injected volume was estimated to be around 10–20 nl, as measured in mineral oil. Without applying pressure, there was no apparent leakage of intrapipette solution since there was no leakage of green color and no change in cortical responses. The staining by fast green was monitored under the surgical microscope, which spread fast under the injection pressure and covered a cortical area with a radius of 500–600 μm at the end of the injection. This also means that the initial concentration of injected cocktail will be quickly diluted by about 50 folds, as estimated from the change in volume. Experiments are normally completed within 30 minutes after drug injection with one drug experiment performed in each animal preparation. Cortical responses largely recovered 7 hours after the injection, likely due to the slow diffusion of drugs in the cortex[13].

In vivo whole-cell recording

Whole-cell recordings[25–27,33,36,37] were obtained from neurons located at 500–700μm beneath the cortical surface, corresponding to the input layers of the auditory cortex[38]. For voltage-clamp recording, the patch pipette (4–7 MΩ) contained (in mM): 125 Cs-gluconate, 5 TEA-Cl, 4 MgATP, 0.3 GTP, 10 phosphocreatine, 10 HEPES, 1 EGTA, 2 CsCl, 2 QX-314, pH 7.2, and 0.5% biocytin. The whole-cell and pipette capacitance were completely compensated and the initial series resistance (20–50MΩ) was compensated for 50–60% to achieve effective series resistance of 10–25 MΩ. Signals were filtered at 5 kHz and sampled at 10 kHz. For current clamp recording to examine spikes, the same patch pipette was used, containing (in mM): 125 K-gluconate, 4 MgATP, 0.3 GTP, 10 phosphocreatine, 10 HEPES, 1 EGTA, pH 7.2, and 0.5% biocytin. Histological staining of the recorded cells[39–41] after recording indicates that the whole-cell recording method under our current condition biasedly sampled pyramidal neurons. In this study, the measured membrane potentials of the recorded neurons ranged from −61 to −72 mV with a mean of −63.8 mV.

To obtain tone-evoked excitatory inputs, the cells were clamped directly at −70mV, which is around the reversal potential of inhibitory currents (Ei) as also described in our previous studies[25,27,33]. Cortical cells can be reasonably clamped before and after cocktail application with clamping deviation within around ± 5 mV(see Supplementary Information Part 2). For a few cases when both excitatory and inhibitory TRFs were obtained before cortical silencing, we derived the excitatory synaptic conductance Ge(t) [25–27,29, 33,41,42] according to $I(t, V) = Gr(V-Er) + Ge(t)(V-Ee) + Gi(t)(V-Ei)$, where V is the clamping voltage, Gr is the resting conductance, Er is the resting potential; Ee and Ei are the reversal potentials for excitatory and inhibitory synaptic currents, respectively; and I(t, V) is the current amplitude under V, and V (t) is given by $V(t) = Vc - Rs*I(t)$, where Rs was the effective series resistance and Vc is the clamping voltage applied. The liquid junction potential is estimated to be 12 mV. We found that varying Ei values between −65 and −75 mV, did not change the conclusion of this study.

Data analysis

Tone-evoked excitatory synaptic or membrane potential responses were identified according to their onset latencies and peak amplitudes. Only responses with the onset and peak occurring within 7–30 ms from the onset of tone stimulus, and with peak amplitude of at least three folds of standard deviation of baseline fluctuation were considered tone-evoked responses. The response onset latency was taken as the time point in the rising phase of the response curve, where the amplitude change was two folds of standard deviation of baseline fluctuation[25]. The boundaries of synaptic TRFs were defined according to the consistency of tone-evoked responses in 2–4 repetitions, and the continuity of responses with the change of frequency and intensity. For color maps of synaptic TRFs, repetitions were averaged, and only the pixels within the determined TRF boundary were labeled[27,33].

The estimated membrane potential responses (Vest) for the voltage-clamp recordings before the drug application were derived using $Vest(t) = (GrVr + Ge(t)Ee + Gi(t)Ei)/(Gr(t) + Ge(t) + Gi(t))$, where Vr is the resting membrane potential. Since Gi was not determined for most of the cells in this study, we derived the membrane potential changes caused by excitatory inputs alone, and estimated the spike threshold at 20 mV above the resting membrane potential.

To correct the non-specific effect of the cocktail application, we averaged tone-evoked responses at the intensity threshold of synaptic TRFs before and after cortical silencing. We have assumed that these responses were mostly contributed by monosynaptic thalamic inputs. The relative reduction in their amplitudes (r) can be largely explained by the changes in input and series resistances after cocktail application (see Supplementary Information Part 2 for detailed calculation), and thus is used as a reflection of non-specific effects of cocktail

application. The amplitude of each response was then normalized by a correction factor of 1/(1−r). It is worth noting that varying the correction factor by ± 25% does not qualitatively change the conclusion of this study.

Supplementary Material

Refer to Web version on PubMed Central for supplementary material.

Acknowledgements

This work is supported by grants to L.I.Z. from NIH/NIDCD, Searle Scholar Program, the Klingenstein Foundation, and the David and Lucile Packard Foundation.

References

1. Reid RC, Alonso JM. Specificity of monosynaptic connections from thalamus to visual cortex. Nature 1995;378:281–284. [PubMed: 7477347]
2. Ferster D, Chung S, Wheat H. Orientation selectivity of thalamic input to simple cells of cat visual cortex. Nature 1996;380:249–252. [PubMed: 8637573]
3. Chung S, Ferster D. Strength and orientation tuning of the thalamic input to simple cells revealed by electrically evoked cortical suppression. Neuron 1998;20:1177–1189. [PubMed: 9655505]
4. Miller LM, Escabi MA, Read HL, Schreiner CE. Functional convergence of response properties in the auditory thalamocortical system. Neuron 2001;32:151–160. [PubMed: 11604146]
5. Bruno RM, Sakmann B. Cortex is driven by weak but synchronously active thalamocortical synapses. Science 2006;312:1622–1627. [PubMed: 16778049]
6. Douglas RJ, Koch C, Mahowald M, Martin KA, Suarez HH. Recurrent excitation in neocortical circuits. Science 1995;269:981–5. [PubMed: 7638624]
7. Somers DC, Nelson SB, Sur M. An emergent model of orientation selectivity in cat visual cortical simple cells. J Neurosci 1995;15:5448–65. [PubMed: 7643194]
8. Miller KD, Pinto DJ, Simons DJ. Processing in layer 4 of the neocortical circuit: new insights from visual and somatosensory cortex. Curr Opin Neurobiol 2001;11:488–97. [PubMed: 11502397]
9. Alonso JM, Swadlow HA. Thalamocortical specificity and the synthesis of sensory cortical receptive fields. J Neurophysiol 2005;94:26–32. [PubMed: 15985693]
10. Miller LM, Escabi MA, Read HL, Schreiner CE. Spectrotemporal receptive fields in the lemniscal auditory thalamus and cortex. J Neurophysiol 2002;87:516–527. [PubMed: 11784767]
11. Miller LM, Escabi MA, Schreiner CE. Feature selectivity and interneuronal cooperation in the thalamocortical system. J Neurosci 2001;21:8136–8144. [PubMed: 11588186]
12. Martinez LM, Wang Q, Reid RC, Pillai C, Alonso JM, Sommer FT, Hirsch JA. Receptive field structure varies with layer in the primary visual cortex. Nat Neurosci 2005;8:372–379. [PubMed: 15711543]
13. Fox K, Wright N, Wallace H, Glazewski S. The origin of cortical surround receptive fields studied in the barrel cortex. J Neurosci 2003;23:8380–8391. [PubMed: 12968000]
14. Kaur S, Lazar R, Metherate R. Intracortical pathways determine breadth of subthreshold frequency receptive fields in primary auditory cortex. J Neurophysiol 2004;91:2551–2567. [PubMed: 14749307]
15. Zhang Y, Suga N. Corticofugal amplification of subcortical responses to single tone stimuli in the mustached bat. J Neurophysiol 1997;78:3489–3492. [PubMed: 9405567]
16. Chung S, Ferster D. Strength and orientation tuning of the thalamic input to simple cells revealed by electrically evoked cortical suppression. Neuron 1998;20:1177–1189. [PubMed: 9655505]
17. Volgushev M, Vidyasagar TR, Chistiakova M, Yousef T, Eysel UT. Membrane properties and spike generation in rat visual cortical cells during reversible cooling. J Physiol 2000;522:59–76. [PubMed: 10618152]

18. Villa AE, Rouiller EM, Simm GM, Zurita P, de Ribaupierre Y, de Ribaupierre F. Corticofugal modulation of the information processing in the auditory thalamus of the cat. Exp Brain Res 1991;86:506–517. [PubMed: 1761088]
19. Yamauchi T, Hori T, Takahashi T. Presynaptic inhibition by muscimol through GABAB receptors. Eur J Neurosci 2000;12:3433–3436. [PubMed: 10998126]
20. Porter JT, Nieves D. Presynaptic GABAb receptors modulate thalamic excitation of inhibitory and excitatory neurons in the mouse barrel cortex. J Neurophysiol 2004;92:2762–2770. [PubMed: 15254073]
21. Roerig B, Chen B. Relationships of Local Inhibitory and Excitatory Circuits to Orientation preference maps in ferret visual cortex. Cereb Cortex 2002;12:187–198. [PubMed: 11739266]
22. Marino J, Schummers J, Lyon DC, Schwabe L, Beck O, Wiesing P, Obermayer K, Sur M. Invariant computations in local cortical networks with balanced excitation and inhibition. Nat Neurosci 2005;8:194–201. [PubMed: 15665876]
23. Zhang LI, Bao S, Merzenich MM. Persistent and specific influences of early acoustic environments on primary auditory cortex. Nat Neurosci 2001;4:1123–30. [PubMed: 11687817]
24. Bringuier V, Chavane F, Glaeser L, Fregnac Y. Horizontal propagation of visual activity in the synaptic integration field of area 17 neurons. Science 1999;283:695–699. [PubMed: 9924031]
25. Zhang LI, Tan AY, Schreiner CE, Merzenich MM. Topography and synaptic shaping of direction selectivity in primary auditory cortex. Nature 2003;424:201–205. [PubMed: 12853959]
26. Wehr M, Zador AM. Balanced inhibition underlies tuning and sharpens spike timing in auditory cortex. Nature 2003;426:442–446. [PubMed: 14647382]
27. Tan AY, Zhang LI, Merzenich MM, Schreiner CE. Tone-evoked excitatory and inhibitory synaptic conductances of primary auditory cortex neurons. J Neurophysiol 2004;92:630–643. [PubMed: 14999047]
28. Carandini M, Ferster D. Membrane potential and firing rate in cat primary visual cortex. J Neurosci 2000;20:470–484. [PubMed: 10627623]
29. Anderson JS, Carandini M, Ferster D. Orientation tuning of input conductance, excitation, and inhibition in cat primary visual cortex. J Neurophysiol 2000;84:909–926. [PubMed: 10938316]
30. Priebe N, Ferster D. Direction Selectivity of Excitation and Inhibition in Simple Cells of the Cat Primary Visual Cortex. Neuron 2005;45:133–145. [PubMed: 15629708]
31. Wilent WB, Contreras D. Stimulus-dependent changes in spike threshold enhance feature selectivity in rat barrel cortex neurons. J Neurosci 2005;25:2983–2991. [PubMed: 15772358]
32. Swadlow HA, Gusev AG. Receptive-field construction in cortical inhibitory interneurons. Nat Neurosci 2002;5:403–404. [PubMed: 11967546]
33. Wu GK, Li P, Tao HW, Zhang LI. Nonmonotonic synaptic excitation and imbalanced inhibition underlying cortical intensity tuning. Neuron 2006;52:705–715. [PubMed: 17114053]
34. Winer JA, Miller LM, Lee CC, Schreiner CE. Auditory thalamocortical transformation: structure and function. Trends Neurosci 2005;28:255–263. [PubMed: 15866200]
35. Calford MB, Webster WR. Auditory representation within principal division of cat medial geniculate body: an electrophysiology study. J Neurophysiol 1981;45:1013–1028. [PubMed: 7252528]
36. Moore CI, Nelson SB. Spatio-temporal subthreshold receptive fields in the vibrissa representation of rat primary somatosensory cortex. J Neurophysiol 1998;80:2882–2892. [PubMed: 9862892]
37. Margrie TW, Brecht M, Sakmann B. In vivo, low-resistance, whole-cell recordings from neurons in the anaesthetized and awake mammalian brain. Pflugers Arch 2002;444:491–498. [PubMed: 12136268]
38. Games KD, Winer JA. Layer V in rat auditory cortex: projections to the inferior colliculus and contralateral cortex. Hear Res 1988;34:1–25. [PubMed: 3403382]
39. Horikawa K, Armstrong WE. A versatile means of intracellular labelling: injection of biocytin and its detection with avidin conjugates. J Neurosci Methods 1988;25:1–11. [PubMed: 3146670]
40. Zhu Y, Stornetta RL, Zhu JJ. Chandelier cells control excessive cortical excitation: characteristics of whisker-evoked synaptic responses of layer 2/3 nonpyramidal and pyramidal neurons. J Neurosci 2004;24:5101–5108. [PubMed: 15175379]

41. Hirsch JA, Alonso JM, Reid RC, Martinez LM. Synaptic integration in striate cortical simple cells. J Neurosci 1998;18:9517–9528. [PubMed: 9801388]

42. Borg-Graham LJ, Monier C, Fregnac Y. Visual input evokes transient and strong shunting inhibition in visual cortical neurons. Nature 1998;393:369–373. [PubMed: 9620800]

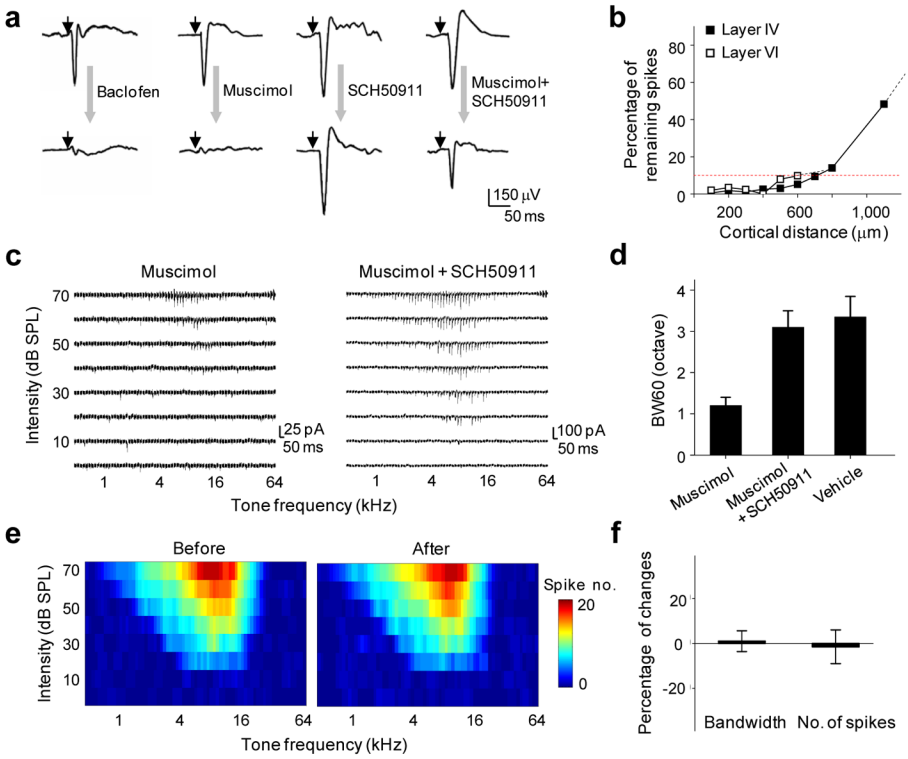

Figure 1.

Specific silencing of local intracortical connections with a cocktail pharmacological method. (**a**) Tone-evoked field potentials recorded in A1 before (top) and after (bottom) cortical injection of muscimol (1 mM), baclofen (1 mM), SCH50911 (1.5mM) or a cocktail of muscimol (1 mM) and SCH50911 (1.5 mM). Small arrow marks the onset of tone stimulus. (**b**) Effective blocking of cortical spikes by the muscimol and SCH50911 (4mM: 6mM) cocktail in both layer 4 and layer 6 within a horizontal distance of 500 μm from the injection site (see Methods). Multi-unit tone-evoked spikes were detected by extracellular recordings. Red dot line indicates 90% reduction in spike count. (**c**) Example excitatory synaptic TRFs of A1 neurons obtained shortly after muscimol injection (left) and cocktail injection (right). Each small trace represents the response (recorded at −70mV) to a tone of a particular frequency and intensity. (**d**) Average bandwidth of synaptic TRF measured at 60dB (BW60) in A1 injected with muscimol, cocktail, or vehicle solution (ACSF). Bar is s.d. (**e**) Spike TRF (average of four repetitions) for a recording site in the MGBv before and after cortical injection of the cocktail. Color represents the number of spikes evoked by a tone stimulus. (**f**) Percentage change in the bandwidth and spike count for tone evoked spikes (measured at 60 dB) in the MGBv before and after cortical cocktail application (*n* = 6 sites). Bar = s.d.

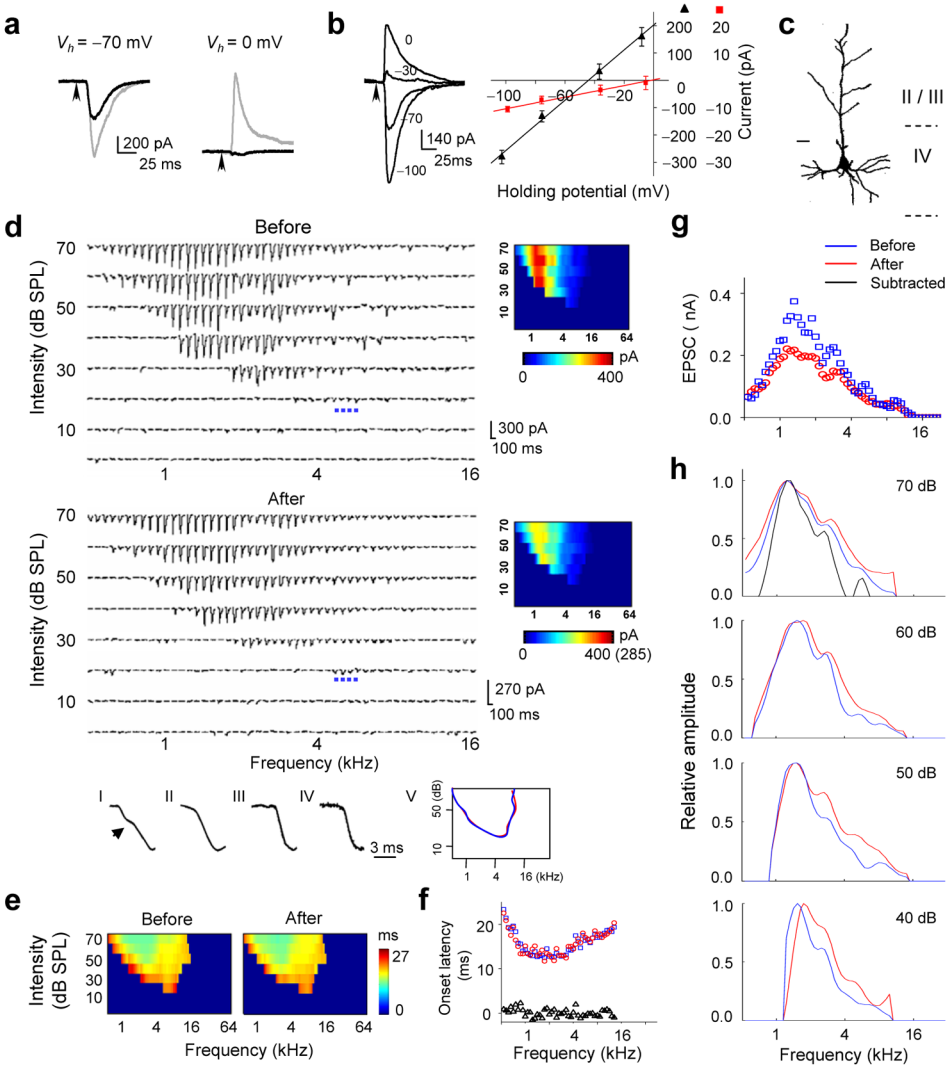

Figure 2.

Changes in excitatory synaptic TRF after local cortical silencing. (**a**) Excitatory (left) and inhibitory (right) synaptic currents evoked by a tone of 1.5 kHz and 70 dB before (gray) and after (black) cocktail application. (**b**) Left, synaptic currents (average of five repeats) evoked by a tone of 1.9 kHz and 70 dB recorded at different holding potentials. Right, *I* –*V* curves (*V* is corrected) for synaptic currents averaged within a 20–22.5 ms window after the stimulus onset (black) and 0–1 ms window after the response onset (red). (**c**) Morphology of this recorded cell. Bar, 20 μm. (**d**) TRF of excitatory synaptic currents before (average of two repeats) and after (four repeats) silencing. Blue dots mark the responses at the intensity threshold (20 dB). The color maps show the average amplitudes. Number in the bracket indicates the original scale before correction. Bottom, **I–IV**, the rising phase of average synaptic response to a 1.3 kHz tone at 60 dB (I/II) or a 5.6 kHz tone at 20 dB (III/IV) before (I/III) and after (II/IV) cortical silencing. (**e**) Color map of onset latencies of evoked excitatory currents. (**f**) Onset latencies (at 70 dB) before (blue) and after (red) cocktail application. Triangle represents the difference. (**g**) Amplitudes of responses before (blue) and after (red) cocktail application at 70 dB. (**h**) Tuning curves of excitatory currents at four different tone intensities. The black line represents the tuning curve of subtracted responses (before minus after).

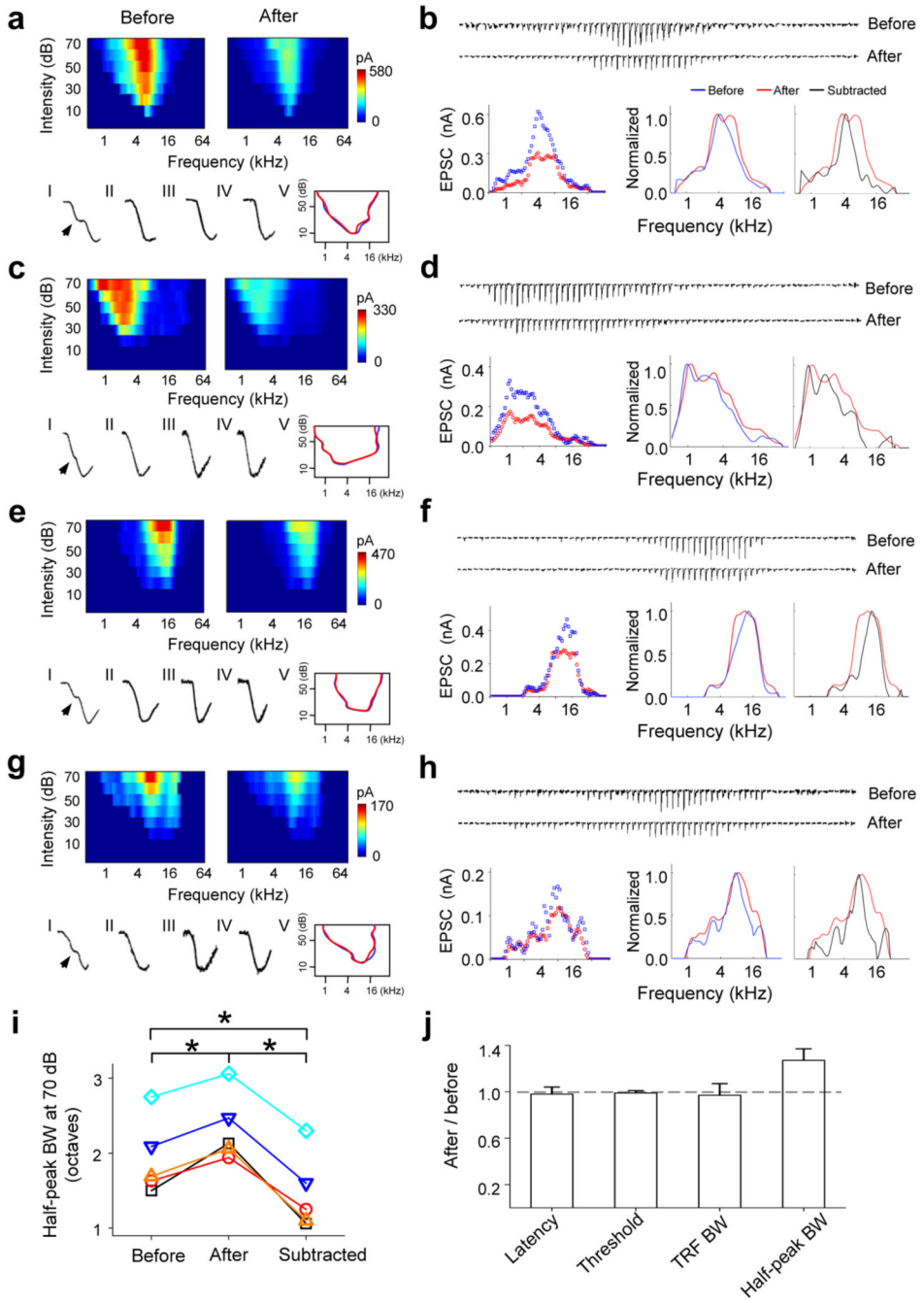

Figure 3.

Intracortical inputs are more sharply tuned than thalamocortical inputs. (**a**–**h**) Change in excitatory synaptic TRF in another four cells. **a, c, e, g**, Top, color maps represent the excitatory synaptic TRF before and after cocktail application. Bottom, kinetics of the rising phase of synaptic currents (1–IV). The curved line outlines the boundary of synaptic TRF before (blue) and after (red) cocktail application (V). Data are presented in the same way as in Fig. 2. **b, d, f, h,** Top, excitatory synaptic currents evoked by tones (at 70 dB) of different frequencies before and after cocktail application. The amplitudes of currents after application are corrected. Bottom, excitatory tuning curves at 70 dB before (blue) and after (red) cortical silencing. Data are presented in a similar manner as in Fig. 2. Black lines are for the subtracted inputs. (**i**) Half-

peak bandwidths of tuning curves at 70 dB for total excitatory inputs (before), thalamic inputs (after) and intracortical inputs (subtracted). Data points from the same cell are connected with lines ($n = 5$, paired t-test, * $P < 0.01$). (**j**) Average ratio of onset latency, intensity threshold of excitatory synaptic TRF, bandwidth at 10 dB above the intensity threshold (TRF BW), and half-peak bandwidth of tuning curve at 70 dB (half-peak BW) between after and before values. Bar = s.d.

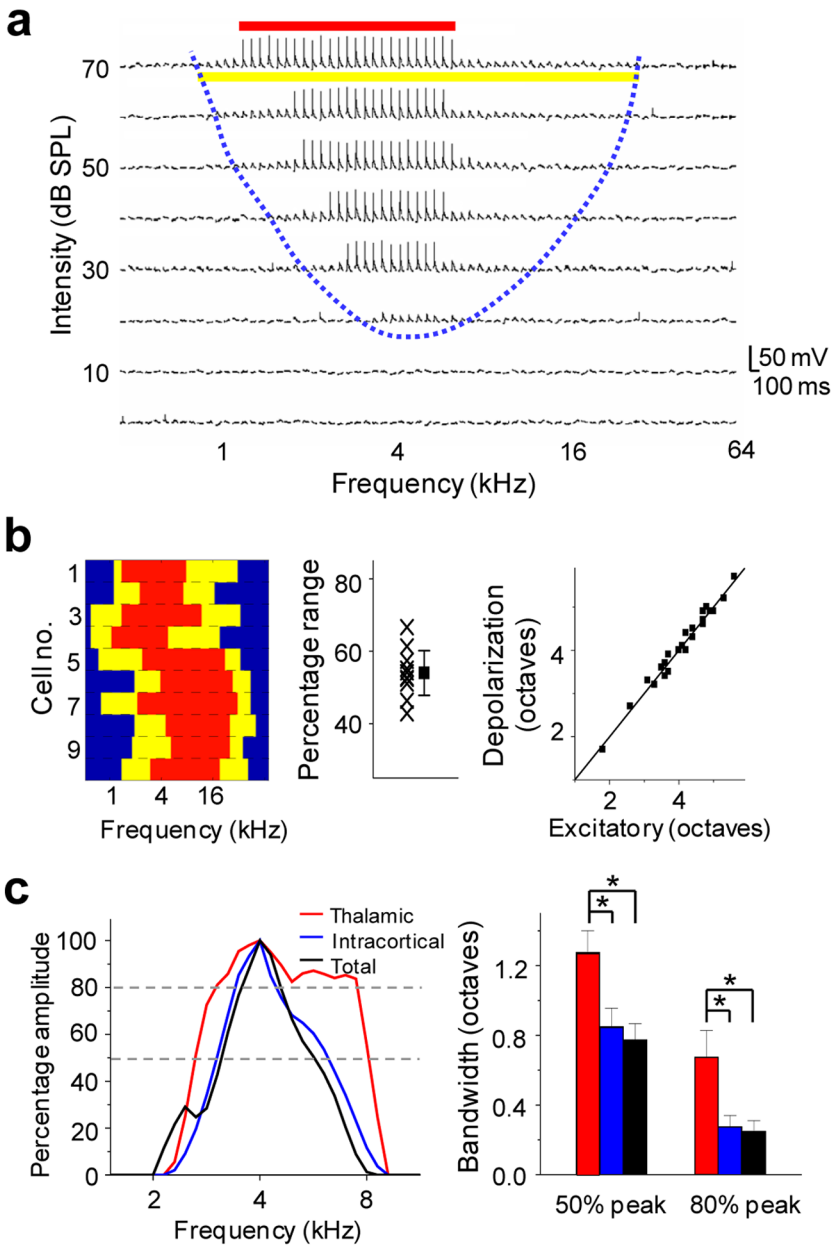

Figure 4.

Similarly tuned intracortical inputs sharpen the frequency tuning curve in layer 4. (**a**) Membrane potential responses to tones of various frequencies and intensities, recorded under current clamp from a representative A1 neuron. Blue dashed line delineates the boundary for the TRF of tone-evoked membrane depolarizations. The yellow and red lines indicate the frequency range (at 70 dB) for subthreshold and spike responses respectively. (**b**) Left, frequency range for subthreshold (yellow) and spike (red) responses at 70 dB of 10 cells detected with current-clamp recording. Middle, percentage frequency range for spike responses within the range for membrane potential responses. Each cross represents one cell. The square represents the average of all cells (± s.d.). Right, for 24 cells in which both voltage-clamp and current-clamp recordings were obtained, the frequency range (at 70 dB) of membrane depolarizations (ordinate) matches well with that of excitatory synaptic currents (abscissa). (**c**) Left, normalized tuning curves after thresholding within the estimated suprathreshold

response range for total excitatory input (black), thalamocortical (red) and intracortical (blue) input in a cell. Right, average bandwidths at 50% and 80% peak amplitude of “suprathreshold” tuning curves (n = 5 cells, paired t-test, * $P < 0.03$). Bar = s.d.